

Observability of the effects of curl-free magnetic vector potential on the macroscale and the nature of the ‘transition amplitude wave’

RAM K VARMA

Physical Research Laboratory, Navrangpura, Ahmedabad 380 009, India
E-mail: ramkvarma@gmail.com

MS received 25 June 2009; revised 4 November 2009; accepted 17 November 2009

Abstract. We discuss here the prediction, based on a formalism by the author, on the observable effects of a curl-free magnetic vector potential on the macroscale as against the microscale of the Aharonov–Bohm effect. A new quantum concept – the ‘transition amplitude wave’ – postulated in the formalism has already been shown to exhibit matter wave manifestations in the form of one-dimensional interference effects on the macroscale. It was predicted by the formalism that the same entity would lead to the detection of a curl-free magnetic vector potential on the macroscale. We describe here the manner of generation of this quantum entity in an inelastic scattering episode and work out an algorithm to observe this radically new phenomenon, the detection of a curl-free magnetic vector potential on the macroscale. We determine the various characteristic features of such an observation which can then be looked for experimentally so as to verify the predicted effect, establishing thereby the physical reality of the new quantum entity, and to fully validate the formalism predicting it. It is also shown that this ‘transition amplitude wave’ can be regarded as a novel kind of ‘quasiparticle’ excited in the charged particle trajectory as a consequence of the scattering episode.

Keywords. Curl-free vector potential; macroscale quantum effects; transition amplitude wave.

PACS Nos 03.65.Ta; 41.75.-i; 41.85.-p

1. Introduction

The Aharonov–Bohm (AB) effect [1], as the observability of the effects of a curl-free magnetic vector potential, is now too well known, and has been demonstrated experimentally by Chambers [2] using a magnetic whisker, more definitively by Tonomura *et al* [3] using a microtoroidal solenoid and by many others subsequently too numerous to recount here. The AB effect is essentially a quantum effect, where the detection of the curl-free vector potential occurs through the interference phenomena, as a ‘fringe shift’ in the double slit interference experiment, for example.

We shall discuss here an entirely new effect of the above-mentioned observability (of the (curl-free) vector potential) on the macroscale as against the microscale of the AB effect. Such an effect will appear to manifestly contravene the currently accepted conceptual framework which does not admit, as per the Lorentz equation, any effect that a curl-free vector potential could have on the dynamics of a charged particle on the macroscale, and hence its detection. Such an observation has been predicted by a formalism developed by the author in a series of theoretical investigations [4–7]. These investigations have led to the formulation of a new quantum entity designated as the ‘transition amplitude wave’. The evolution and development of these ideas over the years have been presented in a recent review [8].

The equations obtained and explored in refs [4–6] over the years have been the cornerstone of the new concepts that we would like to explain in this paper. These are one-dimensional Schrödinger-form equations (eq. (1) below) which have a very large action – the gyroaction – for the particle in a magnetic field ($\mu \sim 10^8 \hbar$) in the role of \hbar . By virtue of the largeness of the action, and the probability amplitude nature of the functions that are governed by these equations, they predict the existence of one-dimensional matter wave interference effects on the macroscale. (These effects have indeed been observed subsequently [9–11]). The concept of the ‘transition amplitude wave’ as a new quantum entity referred to above in fact flows from these equations.

The derivation of these equations in ref. [6] which used the Schrödinger equation (in the path integral representation), enabled the inclusion of a curl-free magnetic vector potential which, as can be seen in eq. (1) appears in the same manner as in the quantic-Schrödinger equation. This then leads to the prediction by these equations of an even more spectacular effect, namely, the detection (in one dimension) of the curl-free magnetic vector potential on the macroscale. Apparently, defying the current wisdom on the observation of curl-free vector potential, which has so far been prejudiced by the Aharonov–Bohm effect, this novel effect has indeed been observed as reported in [12]. Clearly this is entirely heterodox to the canonical understanding of the observability of a curl-free vector potential *à la* Aharonov–Bohm which is a microscale quantum effect and requires a multiply-connected domain with a minimum of two dimensions.

These equations also predict one-dimensional macroscale matter wave interference effects (already observed and reported in refs [9–11]) which correspond to a wavelength with \hbar independent expression $\lambda_m = (2\pi v/\Omega)$, where v is the electron velocity ‘parallel’ to the magnetic field, and $\Omega = eB/mc$ is the electron gyrofrequency in the magnetic field B . For typical experimental parameters, the energy $\mathcal{E} \sim 1$ keV and magnetic field $B \sim 100$ G, $\lambda_m \sim 5$ cm, a surprisingly large (macroscale) wavelength for a matter wave!!

As will be explained later in this paper (§§4 and 5), these observations do not constitute a defiance of the canonical conceptual framework because the observed effects are not exclusive, but inclusive of well-known quantum effects. That is, they represent additional, completely new quantum effects not unravelled so far, to the best of the author’s knowledge that are on the macroscale and which owe their existence to this new quantum entity – the ‘transition amplitude wave’.

The objective of this paper is thus two-fold: One, to explain the nature of this quantum entity and its relationship with quantum formalism so as to understand its macroscale character *vis-á-vis* the microscale character of quantum mechanics in the form of de Broglie waves; its manner of generation, and its interesting properties and ramifications. Two, to understand the role of this entity in the observation of the curl-free vector potential on the macroscale and to work out, using this formalism, additional crucial and distinct features relating to this observation, as against those of the AB effect. These could be looked for experimentally so as to further substantiate the physical reality of the transition amplitude wave (TAW).

2. Theoretical framework

We shall begin by recapitulating some essential elements of the theoretical formalism which led to the predictions of the above-mentioned effects, thereby motivating the experimental investigations unravelling them. There are two governing constituents which define the dynamics of the TAW and the effects emanating from them. These are: (i) the equation of evolution of the TAW and (ii) its generation mechanism and its origin which provides the ‘initial data’ for its evolution. We discuss these below, and work out their consequences.

2.1 Equation of evolution for the ‘transition amplitude wave’

The dynamics of the ‘transition amplitude wave’, defined above for the charged particle in the presence of an external magnetic field and a curl-free vector potential has been shown by the author in ref. [6] to be governed by a set of Schrödinger-form equations:

$$\frac{i\mu}{n} \frac{\partial \Psi(n)}{\partial t} = \frac{1}{2m} \left(\frac{\mu}{in} \frac{\partial}{\partial x} - \frac{e}{c} A_x \right)^2 \Psi(n) + (\mu\Omega)\Psi(n), \quad (1)$$

where x represents the coordinate along the magnetic field, $\Omega = eB/mc$ is the gyrofrequency in the magnetic field B and $\mu = \frac{1}{2}mv_{\perp}^2/\Omega$ is the gyroaction of the particle for its gyromotion in the magnetic field (v_{\perp} is the magnitude of the component of velocity perpendicular to the magnetic field). Also \hat{A}_x is the component along the magnetic field of a part of the vector potential $\hat{\mathbf{A}}$, which is curl-free, so that $\hat{\mathbf{B}} = \nabla \times \hat{\mathbf{A}} = 0$, while the external magnetic field corresponds to the part of the vector potential \mathbf{A} with non-zero curl, so that $\mathbf{B} = \nabla \times \mathbf{A}$. In eq. (1), the magnetic field \mathbf{B} is taken to be axisymmetric, so that $\mathbf{A} = A_{\theta}\hat{\mathbf{e}}_{\theta}$ and $\hat{\mathbf{A}} = \hat{A}_r\hat{\mathbf{e}}_r + \hat{A}_z\hat{\mathbf{e}}_z$ is a curl-free vector potential, so that $\nabla \times \hat{\mathbf{A}} = 0$.

Equation (1) was obtained in ref. [6] starting from the Schrödinger wave equation in its path integral representation, and the wave amplitudes $\Psi(n)$ represent, as per the derivation, transition amplitudes from a large Landau level numbered N , to $N \pm n$ ($N \gg n > 1$) induced by any perturbation including the inhomogeneity of the external magnetic field, while the energy in the parallel coordinate changes to conserve the total energy. The gyroaction μ is identified as $\mu = N\hbar$, and n in

eq. (1) represents the Landau level interval across which transition occurs. The total transition probability over all values of n is given by

$$\mathcal{P}(x, t) = \sum_n \Psi^*(n)\Psi(n). \quad (2)$$

Since these equations have been derived from Schrödinger equation, they must have a quantum character. Consequently, all the phenomena following from these ought to be regarded as of quantum nature, including the macroscale matter wave interference effects reported in [10,11]. It ought also to be specifically stated that, by the same token, these equations must NOT be regarded as ‘quantum-like’ (an expression which implies merely a mathematical similarity without a quantum content). These are equations with a real quantum content, which do, interestingly, have a Schrödinger form. The reader may, however, be intrigued as to how the results depicting matter–matter wave manifestations on the macroscale in accordance with these equations should be so widely at variance with the microscale matter wave concept characterizing quantum mechanics, the parent formalism. To understand this conundrum one needs to examine closely the derivation in ref. [6] and the meaning of the wave function governed by the resulting equations. The wave function basically describes, as per the derivation, what may be regarded as a ‘quantum modulation’ of the pre-scattering free motion along the field line, which is induced by a transition across the bound Landau states of the perpendicular motion caused by the scattering. This ‘modulation’ itself represents a matter wave with a spatial scale characterized by the Landau level interval spanned by the transition. That such a phenomenon should occur is related to the very nature of quantum mechanics, implying a ‘connectedness’ of the degrees of freedom of a system: A process occurring in one degree of freedom would have effect on others. This comment should help in understanding the nature of this new object. The author is not aware whether such a concept has been advanced earlier.

However, it need not follow, it may be argued, that such a modulation would have observable consequences. It would require a recognition and an active interpretation to that effect. Interpretation is an important logical component of this formalism. Following this, these equations may be called upon to predict the various macroscale matter wave effects, which would follow from the presence of a large action $\mu = N\hbar$ in the role of \hbar .

We shall first indicate how the above-mentioned expression for the macroscale matter wavelength follows from eq. (1). We first notice that the latter equation has a large action $\mu = N\hbar$, $N \gg 1$ in the role of \hbar when compared with the quantum-Schrödinger equation. With the above-mentioned parameters, the gyroaction $\mu = \mathcal{E}_\perp/\Omega = N\hbar$, $N \sim 10^8$, the above equation would correspond to a wavelength $\lambda_m \sim 10^8 \lambda_{dB}$, where λ_{dB} is the de Broglie wavelength. It is shown in Appendix A of this paper how this expression for $\lambda_m = 2\pi v/\Omega$ follows from eq. (1). This is, however, more directly obtained in the Appendix of ref. [10] which was later developed into a more general formalism in ref. [7].

2.2 The generation of the TAW and its origin

As mentioned above, the TAW is generated in the unbound degree of freedom of the system – along the magnetic field in the present case of charged particle dynamics – as a consequence of a total energy conserving inelastic scattering resulting in the excitation of its bound energy levels through an interval n from the initial Landau level number N . It has been shown in ref. [7], using the Feynman path integral formalism, that the transition amplitude for such an excitation is given by

$$\begin{aligned} \hat{\Psi}(x, x_c) &= e^{in\Omega(x-x_c)/v} \mathcal{M}(N \rightarrow N+n), \quad x > x_c, \\ &= 1, \quad \text{for } x < x_c, \end{aligned} \quad (3)$$

where $\mathcal{M}(N \rightarrow N+n)$ denotes the matrix element for the above transition in the first Born approximation and x_c is the centre of the scattering potential, with Ω and v as defined above. The derivation of (3) in ref. [7] consists essentially of taking an ‘overlap’ of the post-scattering final state $|N+n, k'\rangle$ with the initial state $|N, k\rangle$ with respect to the microscale variables.

$$\begin{aligned} \hat{\Psi}(n, k) &= \langle N, k | N+n, k' \rangle \mathcal{M}(N \rightarrow N+n) \\ &= e^{i(k'-k)(x-x_o)} \langle N | N+n \rangle \mathcal{M}(N \rightarrow N+n). \end{aligned} \quad (4)$$

An expression for $(k' - k)$ in eq. (4) can be determined from the total energy conservation relation

$$\frac{(\hbar k)^2}{2m} + N\hbar\Omega = \frac{(\hbar k')^2}{2m} + (N+n)\hbar\Omega \quad (5)$$

which yields (using $n \ll N, k' \simeq k$)

$$(k' - k) \simeq \frac{n\Omega}{v} = -\kappa_n. \quad (6)$$

Note that the expression (3) gives directly the expression for the wavelength of the TAW. We note that this expression which is admittedly for a matter wave (because of its quantum origin) is independent of the Planck quantum which leads to its macroscale character.

The expression $\hat{\Psi}(x, x_c)$ defined above constitutes a very crucial result: (a) It represents a one-dimensional matter wave along x with wavelength $\lambda_n = (2\pi v/n\Omega)$ with the integer n describing the harmonic wave numbers as established experimentally in refs [10,11]. (b) It serves as an ‘initial data’ for eq. (1) which would evolve the TAW from then on, and most importantly (c) the centre of scattering potential x_c is the point of origin of the TAW. That is, there arises a TAW only subsequent to scattering, and there is none prior to that. This is what is expressed by the two lines of eq. (3).

This (last) important and distinct feature of the TAW will be seen to be rather crucial in the prediction and subsequent observation of the curl-free vector potential on the macroscale. We shall discuss in §§3 and 4 the important role that this feature plays in the observability of the latter.

3. Theoretical algorithm and the methodology of experimentation

To fix ideas with respect to the experimentation to be carried out, consider a stream of charged particles (electrons) emitted from an electron gun and moving along a magnetic field with a parallel velocity v_{\parallel} and a perpendicular velocity v_{\perp} which, along with the magnetic field B , defines the gyroaction $\mu = \frac{1}{2}mv_{\perp}^2/\Omega$, $\Omega = eB/mc$. Note that the pitch angle of injection $\delta = \tan^{-1}(v_{\perp}/v_{\parallel})$ inevitably has a small spread, so would μ around a mean μ_o , $\delta\mu = (\mu - \mu_o)$, as also the Landau quantum number $N = N_o + \delta N$.

This stream of particles can thus be described as a wavepacket with de Broglie waves along the magnetic field, and Landau states perpendicular to it centred around the state $|N_o, k_o\rangle$, k_o being the central de Broglie wave number. Consider that this stream encounters a planar grid of scatterers normal to the field at a linear position x_g along the field. The scattering will, in general, lead to a transition from $|N_o, k_o\rangle$ to the neighbouring states $|N, k\rangle = |N_o + n, k_o + \kappa\rangle$, with $n \ll N_o$ and $\kappa \ll k_o$. The ‘transition amplitude wave’ generated at the position of the grid is given by eq. (3) above with the grid position x_g replacing x_c .

This equation basically states a very important fact, that prior to the scattering episode at $x = x_g$, the dynamics along the magnetic field is governed by the Schrödinger equation in the form of de Broglie waves, while subsequent to that it is governed by the evolution equation (1) for the TAW. This means that the path lengths for the TAW are to be reckoned from the points of their origin. This algorithm has been used to explain successfully the experimental results [11] exhibiting rather interesting macroscale matter wave ‘beats’ obtained with varying positions of the grid. The same algorithm will be used to work out the consequences in the present case (vector potential observation) as well.

Figure 1 depicts a conceptual representation of the proposed experiment: O represents the position of the electron gun source situated at the right end of an evacuated chamber permeated by a (almost uniform) magnetic field B produced by a set of current carrying coils (not shown), P represents the detector plate which would measure the electron current reaching it; Q is the planar movable grid situated at z_g (in a cylindrical coordinate system (r, θ, z)) or equivalently at x_g along the field line coordinate. TS is a toroidally wound solenoid with a rectangular cross-section of length ℓ_o and mean radius r_o . Ideally, it would have the magnetic flux Φ completely trapped within it. This will lead to a vector potential field $\hat{\mathbf{A}}$ in the space around which would be curl-free. The vector potential lines $\hat{\mathbf{A}} = (\hat{A}_r\hat{\mathbf{e}}_r + \hat{A}_z\hat{\mathbf{e}}_z)$ are as shown schematically.

Apart from the grid which acts as a scatterer to generate the TAW, the perpendicular component of the electric field in the electron-gun region also serves as a generator of the TAW as it scatters electrons across the Landau levels while passing across the anode along the magnetic field. The position of the anode thus serves as an origin of the TAW.

The above discussed detection of the curl-free vector potential is a rather subtle effect as against the corresponding quantum AB effect which is relatively straightforward. The former’s macroscale character and one-dimensionality are its unique though heterodox features. However, in both cases the detection occurs through the agency of the corresponding interference phenomenon; with the de Broglie waves

Nature of the transition amplitude wave

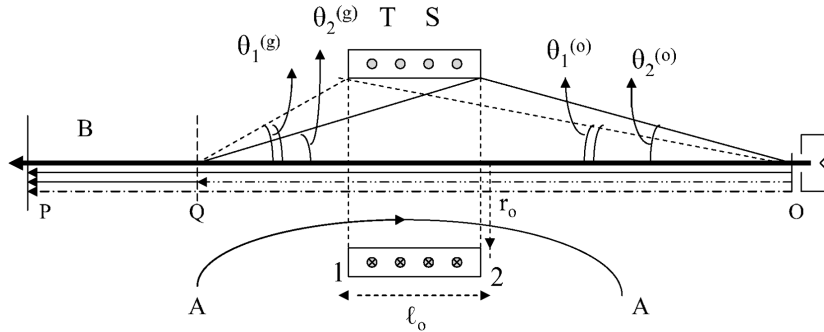


Figure 1. Schematic representation of the experimental arrangement with the toroidal solenoid TS (length ℓ_o , radius r_o), the position of the plate P, of the electron gun O, and the position of the grid Q. The various angles $\theta_1^{(g)}$, $\theta_2^{(g)}$, $\theta_1^{(o)}$ and $\theta_2^{(o)}$ mentioned in the text are as shown. Bold line with an arrow from O to P represents the magnetic field. Full lines from O to P and from Q to P denote the propagation lines of the ‘transition amplitude wave’, while the dash-dotted broken lines from O to P and from O to Q represent the propagation lines of the de Broglie waves along the magnetic field. The curved line AA represents a typical field line of the curl-free vector potential produced by the toroidal solenoid TS.

in the AB case, and the TAW in one dimension in the present case which involves the phase of the TAW wave function. The interference phenomenon here is the one dimensional one reported in refs [9–11] and the detection of the vector potential would occur through a ‘fringe shift’ arising due to the presence of \hat{A}_x in the phase of the TAW governed by eq. (1).

The amplitude $\Psi_1^{(n)}$ at the TAW at $x = x_p$ arriving from x_o (the gun-anode position) is, from eq. (1), given by

$$\Psi_1^{(n)}(x_p) = \alpha_1 \exp \left[\frac{in}{\mu} \int_{x_o}^{x_p} dx \left(mv + \frac{e}{c} \hat{A}_x \right) \right], \quad (7)$$

where v is the velocity parallel to the magnetic field, given by $v = [2(\mathcal{E} - \mu\Omega)/m]^{1/2}$, \mathcal{E} being the total energy, and the superscript n corresponds to the index n of eq. (1).

Only a fraction of the de Broglie wave amplitude suffers scattering in the anode region of the gun, and the unscattered part of the amplitude travels forward. As it encounters the grid situated at $z = z_g$ between z_o and z_p , the unscattered de Broglie wave arriving at z_g undergoes another (inelastic) scattering by the grid wires (either by grazing encounters or by the image charges) leading to the generation of transition amplitude wave originating at z_g . Note that the notation x represents a position along a field line while z represents a coordinate in the cylindrical coordinate system, (r, θ, z) . The positions of the plate and the grid are thus denoted by z_p and z_g respectively. On the other hand, the positions of the plate and the grid along the field line are denoted by x_p and x_g . The wave amplitude $\Psi_2^{(n)}(x_p)$ at the plate $z = z_p$ for the TAW originating at the grid, is given by

$$\Psi_2^{(n)}(x_p) = \alpha_2 \exp \left[\frac{in}{\mu} \int_{x_g}^{x_p} dx \left(mv + \frac{e}{c} \hat{A}_x \right) \right]. \quad (8)$$

The line integrals in eqs (7) and (8) are respectively along the paths (x_o, x_p) and (x_g, x_p) over which the TAW propagates after its generation at x_o and x_g . In figure 1 the solid lines from x_o to x_p and from x_g to x_p represent propagation lines of the TAW whereas the broken line from x_o to x_g represent propagation line of the de Broglie wave. However, as will be discussed in §5, the TAW is essentially a structure which rides along the trajectory with the de Broglie wave as a sort of ‘carrier wave’. The total probability current density at the plate position x_p is then given to be proportional to the total probability density

$$\begin{aligned} |\Psi^{(n)}(x_p)|^2 &= |\Psi_1^{(n)}(x_p) + \Psi_2^{(n)}(x_p)|^2 \\ &= \alpha_1^2 + \alpha_2^2 + 2\alpha_1\alpha_2 \cos \left[\frac{n}{\mu} \int_{x_o}^{x_g} dx \left(mv + \frac{e}{c} \hat{A}_x \right) \right]. \end{aligned} \quad (9)$$

The interference (cosine) term in eq. (9) then corresponds to the interference between the transition amplitude waves generated at z_o and z_g represented respectively by eqs (7) and (8). Note that the line integral over the vector potential \hat{A}_x in the argument of the cosine term is over the ‘open’ path (x_o, x_g) , which is the path difference between the paths (x_o, x_p) and (x_g, x_p) (represented by solid lines in figure 1) traversed by the TAW.

In view of the small spread $\Delta\mu$ in the injected μ values around a mean $\bar{\mu}$, eq. (9) needs to be integrated over this spread. This is analogous to integrating the plane-wave function of a dispersive wave over a spread in the wave number Δk . This leads to the concept of ‘group-velocity’ of the group of waves. A similar group-like property is expected to emerge here as well. Rewriting eq. (9) in the form

$$\begin{aligned} |\Psi^{(n)}(x_p, \mu)|^2 &= |\Psi_1^{(n)}(x_p) + \Psi_2^{(n)}(x_p)|^2 \\ &= \alpha_1^2 + \alpha_2^2 + 2\alpha_1\alpha_2 \cos \left[\frac{1}{\mu} \left\{ n \int_{x_o}^{x_g} dx \left(mv + \frac{e}{c} \hat{A}_x \right) - 2\pi k\mu \right\} \right], \end{aligned} \quad (10)$$

and integrating it over the spread in μ , we obtain

$$\begin{aligned} |\Psi^{(n)}(x_p, \bar{\mu})|^2 &= \alpha_1^2 + \alpha_2^2 \\ &+ 2\alpha_1\alpha_2 \cos \left[\frac{1}{\bar{\mu}} \left\{ n \int_{x_o}^{x_g} dx \left(m\bar{v} + \frac{e}{c} A_x \right) - 2\pi k\bar{\mu} \right\} \right] \times F(X), \end{aligned} \quad (11)$$

where

$$F(X) = \exp \left[- \left(\frac{1}{2\beta\bar{\mu}} \right)^2 X^2 \right], \quad (12)$$

and

$$X \equiv \left[n \int_{x_o}^{x_g} \frac{\Omega dx}{\bar{v}} - 2\pi\ell \right], \quad (13)$$

Nature of the transition amplitude wave

if the distribution $f(\mu)$ in μ is assumed to be a Gaussian of the form

$$f(\mu) = \frac{\beta}{\sqrt{\pi}} e^{-\beta^2(\mu-\bar{\mu})^2}. \quad (14)$$

The details are given in Appendix A. Here \bar{v} is the ‘parallel’ velocity corresponding to the mean value $\bar{\mu}$ and $\bar{v} = [2(\mathcal{E} - \bar{\mu}\Omega)/m]^{1/2}$. The interference term in (11) has the factor $F(X) = \exp\left[\left(-\frac{1}{2\beta\bar{\mu}}\right)^2 X^2\right]$, with X given by (13). This implies that the amplitude of the interference term would be maximum wherever $X = 0$, that is,

$$n \int_{x_o}^{x_g} \frac{\Omega dx}{\bar{v}} = 2\pi\ell, \quad \ell = 1, 2, 3, \dots, \quad (15)$$

where, as discussed in Appendix A, $n\Omega/\bar{v}$ may be regarded as a ‘group’ macroscale matter wave number (see ref. [10], in particular, its Appendix). Equation (15) expresses the condition that the cumulative phase difference between the points x_o and x_g is an integral multiple of 2π . One would thus get a series of interference maxima given by eq. (15); the smaller the value of $\beta\bar{\mu}$, the sharper is the maxima. This factor also leads to the amplitude term becoming rapidly small if X departs from zero when $\beta\bar{\mu}$ is small. A small enough $\bar{\mu}$ would ensure the above relation (15).

The condition (15) can be written in the form:

$$n\bar{\Omega}_g L_g = 2\pi\ell v_o, \quad \ell = 1, 2, 3, \dots, \quad (16)$$

where

$$\bar{\Omega}_{g(p)} = \frac{\Omega_0}{L_{g(p)}} \int_{z_o}^{z_{g(p)}} \frac{b(x)(dx/dz)dz}{\sqrt{1 - b(x) \sin^2 \delta}}, \quad (17)$$

and $v_o = (2\mathcal{E}/m)^{1/2}$ and $b(x) = B(x)/B_o$, B_o being the magnetic field at the point of injection. We have denoted $\bar{\Omega}_g$ in (16) and (17) with the subscripts $g(p)$ to indicate that it is an average over the length $L_{g(p)} = (z_{g(p)} - z_o)$, the gun-grid (plate) distance along the field line. It may be noted from eq. (16) that if for a given v_o , we change the length L_g to L_p , this would require that the magnetic field be changed to $\bar{B}_p = \bar{B}_g(L_g/L_p)$ so as to satisfy the condition for the occurrence of any order ℓ of the interference maximum. This means that we have

$$n\bar{\Omega}_p L_p = n\bar{\Omega}_g L_g = 2\pi\ell v_o, \quad \ell = 1, 2, 3, \dots \quad (18)$$

Now the cosine factor in eq. (11) leads for its maxima to the condition

$$n \int_{x_o}^{x_g} dx \left(m\bar{v} + \frac{e}{c} \hat{A} \right) = 2\pi k \bar{\mu}, \quad k = 1, 2, 3, \dots, \quad (19)$$

describing a series of interference maxima with respect to the variation of the vector potential. It is through the argument of the cosine function that the effect of the vector potential would be detectable. As mentioned earlier, the integral in (19) is

over the ‘open path’ (x_o, x_g) . This is in contrast with the canonical quantum case (the AB effect) where the interfering paths enclose the flux topologically, so that one has the circuit integral $\oint \mathbf{A} \cdot d\ell = \Phi$. The one-dimensional open path difference (x_o, x_g) is the unique feature of the present case which involves the scattering generated transition amplitude waves interfering with each other.

Equations (18) and (19) now constitute the defining equations for the detection on the macroscale of the curl-free vector potential. While eq. (18) locates the position of the maximum of the one-dimensional macroscale matter wave interference, in terms of the gun–grid distance and the corresponding magnetic field for a given electron energy, eq. (19) determines the condition that the interference maximum ‘returns’ after every 2π phase change as a consequence of the variation of the vector potential field in space through which electrons propagate.

The curl-free vector potential (\hat{A}_r, \hat{A}_z) is produced by the flux confined in a toroid (radius r_o , width ℓ_o). This is calculated in the Coulomb gauge with the flux Φ as its source with the boundary conditions $A_z \rightarrow 0$ for $|z| \rightarrow \infty$. With such an expression for A_z , the line integral $\int_{x_o}^{x_g} A_x dx$ can then be evaluated along a path connecting x_o and x_g which passes through the toroid (to correspond to the electron trajectory from the gun to the plate) rather than the one around the toroid externally. Clearly, the latter path is not available to the electrons to reach the plate since the toroidal solenoid is placed external to the glass chamber, and moreover the electrons are tied to the magnetic field. This yields $\int_{x_o}^{x_g} A_x dx = \int_{z_o}^{z_g} A_z dz = G\Phi$, where G is the geometrical factor which is determined by the above-mentioned choice of the path. The above line integral may not appear to be manifestly gauge invariant, because while the flux Φ indeed is, the factor G may be argued not to be so. But since no path other than the one specified above is available to the electrons between x_o and x_p , there is no ambiguity left about the factor G . However, to be more explicit, one may plug a gauge transformation $A_x \rightarrow A'_x = A_x + (\partial\Lambda/\partial x)$ in the above line integral. Since the latter appears in the argument of the cosine factor, it is easily seen that the term $\partial\Lambda/\partial x$ induces a phase change in the latter argument, which involves the value of Λ only at the end-points of the open-path (x_o, x_g) . Since Λ defining the gauge transformation is an arbitrary function, the phase change is of little physical significance and may be chosen to vanish. The Coulomb gauge can then be chosen, without loss of generality, to evaluate the above line integral. By contrast, the circuit integral $\oint A_\ell d\ell$ which appears in the AB effect, is manifestly gauge invariant, being equal to the total flux Φ . Equation (19) then yields the following condition:

$$n \left(\int_{x_o}^{x_g} mv_x dx + \frac{e}{c} G\Phi \right) = 2\pi k\mu; \quad k = 1, 2, 3, \dots, \tag{20}$$

where the geometrical factor G as defined above, depends on the dimensions of the torus and the location of the path (x_o, x_g) for the line integral; and $G < 1$ because the open path (x_o, x_g) subtends only a fraction of the total angle 2π corresponding to the closed path around the toroid which yields the total flux Φ .

The experiment is typically carried out by tuning the external magnetic field for a given electron energy \mathcal{E} , and the gun–grid distance L_g , so as to be on an interference maximum corresponding to a particular value of ℓ in (16). This would be indicated by the appearance of maximum detector current. The effect of the

curl-free vector potential is then observable through the cosine factor in (11) whose argument carries the vector potential \hat{A}_x through the line integral, and thereby the flux Φ . Thus, as the flux Φ is varied in the toroidal solenoid by varying the current in it, the cosine factor would oscillate leading to an oscillation of the interference term. This essentially corresponds to the ‘return’ of the interference maximum for every 2π change of phase induced by the variation of the vector potential. This is, therefore, the manner in which the curl-free vector potential \hat{A} is envisaged to be detected, and has indeed been detected as reported in [12].

Since the velocity \bar{v} is not affected by the change in the vector potential, we get from (20) the following condition for the differences $\Delta\Phi$ and Δk :

$$n \frac{e}{c} G \Delta\Phi = 2\pi(\Delta k) \bar{\mu}, \quad \Delta k = 1, 2, 3, \dots \quad (21)$$

for the maxima of the cosine factor. It may be remarked at this juncture that the arbitrary phase term $[(\Lambda(x_g) - \Lambda(x_o))]$ arising out of the gauge transformation discussed above would, in any case, stand annihilated in eq. (21) which involves only the differences $\Delta\Phi$ and Δk .

Note that the integer n occurring in eq. (16) specifies for its different values $n = 1, 2, \dots$, various sets of interference maxima (a set corresponds to $\ell = 1, 2, 3, \dots$). We redefine it as \hat{n} to distinguish it from n occurring in eq. (21). As shown in [11], the maxima for the set $\hat{n} = 1$, are the largest. For a given energy \mathcal{E} , and L_g , these maxima are obtained by tuning the magnetic field appropriately to correspond to the relation (16) or equivalently to the condition (18). It is essential to incorporate this condition in (21). This is done by dividing it by the former (right (left) hand side of (21) by right (left) hand side of (18)). Using the definition $\bar{\mu} = \frac{1}{2}mv_{\perp}^2/\Omega_o = \mathcal{E} \sin^2 \delta/\Omega_o$ this yields

$$\begin{aligned} n\Delta\Phi &= \hat{n} \frac{c}{2e} (mv_o L_g) \left(\frac{\bar{B}_g}{B_o} \right) \frac{\sin \delta \tan \delta}{G} (\Delta k) \\ &= \hat{n} \frac{c}{2e} \frac{(mv_o L_p)}{G} \left(\frac{\bar{B}_p}{B_o} \right) \sin \delta \tan \delta (\Delta k), \quad \Delta k = 1, 2, \dots, \end{aligned} \quad (22)$$

where eq. (18) is used to substitute for \bar{B}_g in favour of \bar{B}_p through the relation $\bar{B}_g = \bar{B}_p (L_p/L_g)$ to obtain the second row of (22), thus making it independent of $L_g \bar{B}_g$. Here δ is the initial pitch angle of the injected particles at the position of the gun, B_o is the magnetic field at the point of injection and v_o is the speed of the injected electrons.

There are basically three parameters involved in the expression (22) for $\Delta\Phi$: the electron energy \mathcal{E} (through v_o), the pitch angle δ and the geometrical factor (L_p/G). We shall choose $\hat{n} = 1$ as it corresponds to the set with the strongest maxima. It is to be noted that the expression (22) depends only on the ratio (\bar{B}_p/B_o) rather than on the absolute value of the magnetic field anywhere. This constitutes a great simplification from an experimental viewpoint as it is now not necessary to know the absolute value of magnetic field inside the vacuum chamber.

To determine the geometrical factor G for the toroidal solenoid employed, we evaluate the integral $\int \hat{A}_x dx$ with the expression for \hat{A}_x appropriate for the toroidal solenoid (TS) calculated in the Coulomb gauge (refer figure 1 showing the TS, with

the width ℓ_o and mean radius r_o , and the axis of symmetry PQO coinciding with the z -axis). Since the electrons are injected along the magnetic field line coinciding with the axis of symmetry and the pitch angle δ , the integral $\int \hat{A}_x dx$ along the field line is the same as the integral $\int \hat{A}_z dz$.

The curl-free vector potential component \hat{A}_z due to the toroidal solenoid trapping a flux Φ as its source, calculated in the Coulomb gauge with the boundary condition $\hat{\mathbf{A}}(|\mathbf{z}| \rightarrow \infty) = 0$, is given by the expression

$$\hat{A}_z = \frac{\Phi}{\ell_o}(\cos \theta_1 - \cos \theta_2), \tag{23}$$

where θ_1 and θ_2 are the angles, as shown in figure 1 subtended at any position z along the axis by the edges 1 and 2 of the TS. If z_g is the position of the grid Q, and z_o the position of the source O, then the integral $\int_{z_o}^{z_g} A_z dz$ can be shown to be given by

$$\int_{z_o}^{z_g} dz A_z = \Phi \left(\frac{r_o}{\ell_o} \right) \times [\text{cosec } \theta_2^{(g)} - \text{cosec } \theta_1^{(g)} - (\text{cosec } \theta_2^{(o)} - \text{cosec } \theta_1^{(o)})] = G\Phi, \tag{24}$$

where $\theta_1^{(g)}$ and $\theta_2^{(g)}$ are the angles subtended by the edges 1 and 2 of the solenoid ring at the position of the grid Q and $\theta_1^{(o)}$ and $\theta_2^{(o)}$ those at the position O of the electron gun. Thus the geometrical factor G in eqs (20) and (21) can be gleaned from eq. (24).

4. Dependence on the various parameters

The relation (22) which is obtained from the basic equations (11) and (19) involves various parameters such as the energy \mathcal{E} through v_o , the pitch angle δ , and the position x_g of the grid, and that of the source x_o in relation to the toroid, through the geometrical factor G given by (24) which is expressed through the angles $\theta_1^{(g)}, \theta_2^{(g)}, \theta_1^{(o)}$ and $\theta_2^{(o)}$ and the ratio r_o/ℓ_o .

4.1 Dependence on the electron energy

The most obvious of the parameters on which $\Delta\Phi$ depends as per eq.(22), is the electron energy \mathcal{E} . It gives $\Delta\Phi \sim \sqrt{\mathcal{E}}$, since $v_o \sim \mathcal{E}^{1/2}$. In this respect, it is to be noted that the present effect is distinct from the AB effect where no dependence on electron energy exists, and the fringe shift is determined entirely by the enclosed flux – a property referred to as the dispersion-free nature of the effect. This dependence on the energy has already been checked in ref. [12], but could still be repeated with more measurements over a larger range of energy values.

4.2 Dependence on the gun-grid distance

Recall that the wave algorithm given in §3 stipulates that the interference term in the expression (9) is a consequence of interference between the two transition amplitude waves given by (7) and (8). They emanate respectively from the electron gun region and the grid as a consequence of their generation through electron scattering by the electric field and the grid wires. The path difference that is involved in the interference at the plate is thus the gun-grid distance $L_g = (z_g - z_o)$. However, as mentioned above, the gun-grid distance also affects the geometrical factor G and consequently the positions of the maxima and minima in terms of $\Delta\Phi$ of eq. (22) through its dependence on the factor L_p/G . With L_p kept fixed throughout, the interpeak separation for $\Delta\Phi$ would depend inversely on G . Since the expression for G is determined by the line integral $\int_{x_o}^{x_g} dx \hat{A}_x$, it ought to decrease with decreasing $L_g = (x_g - x_o)$. Consequently, $\Delta\Phi$ which depends inversely on G would increase with the decrease of L_g .

It would therefore be important to check this dependence by monitoring the interpeak separation of interference maxima over the entire range of values of L_g from a small value to almost the plate position ($L_g \leq L_p$). An experimental confirmation of the dependence of $\Delta\Phi$ with the variation of the distance L_g will validate the premise that the grid does act as a source of the TAW. A discussion of the dependence of $\Delta\Phi$ on the factor $1/G$ as the grid is moved through the toroidal solenoid from a position close to the plate to the one close to the gun, is given in Appendix B.

In order to be able to compare the theoretically expected dependence of $\Delta^{(1)}\Phi$ on the gun-grid distance L_g or equivalently on the plate-grid distance $D = L_p - L_g$ through the factor $1/G$, we plot $1/G$ at a value D , normalized to its value for a certain $D_o = (2/5)L_p$, letting $L_p = 30$ in arbitrary units. The normalized value $R = [G_{D_o}/G_D]$ is then calculated for various values of D , and plotted against the latter for $\ell_o = 5.8$, and three values of $r_o = 5.6, 5.8$ and 6.0 all in arbitrary units. This shows how sensitive R is to the three close values of r_o . Such a plot is presented in figure 2.

It is noteworthy to see from figure 2 that the ratio R rises rather dramatically for the value of D/L beyond $\frac{1}{2}(L + \ell_o)/L$, that is, as the grid moves across the length of the toroid. The dotted lines drawn parallel to the ordinate denote the location of the planes of the toroid. This implies that the factor G on which R depends inversely, decreases rapidly as the grid moves through the toroid from $D \leq 0.5(L - \ell)$ to $D \geq 0.5(L + \ell)$. However, for distances $0 < D < 0.5(L - \ell)$ the variation of the ratio R is very slight (~ 0.3 over a distance $0 < D < 0.4L = 12$ for $L = 30$) as can be seen from figure 2

When experimentally substantiated, this prediction of the dependence of $\Delta\Phi$ on $1/G$ would be quite striking because it implies that a mere change in the position of the grid (which is usually regarded as a passive element, particularly, as a grounded grid) affects the plate current profile in an unexpectedly drastic manner. This is by far the most crucial dependence whose experimental confirmation will validate, *a fortiori*, the entire formalism of TAW. In fact from the perspective of the conventional view of the experiment as proposed to be performed, the dependence exhibited in figure 2 will be seen to be quite astonishing.

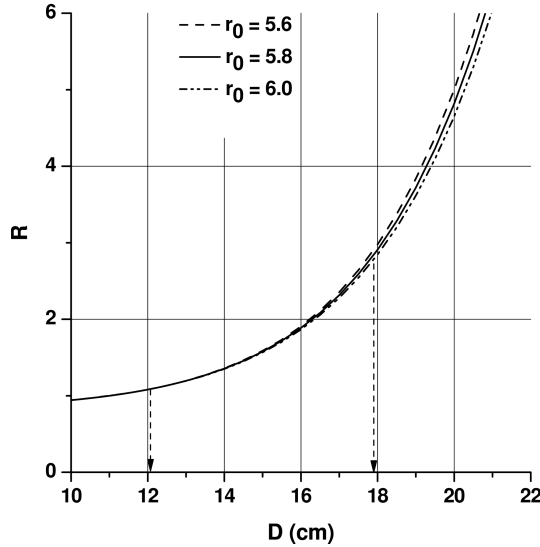


Figure 2. Calculated value of the ratio $R = G_{D_o}/G_D$, the value of $(1/G)$ for $D = (L - L_g)$, normalized to its value for $D = D_o = 0.4L = 12$ (with $L = 30$ arb. units), as a function of D for $\ell_o = 5.8$, and three values of $r_o = 5.6, 5.8, 6.0$. The dotted vertical lines with an arrow indicate the positions of the edges of the toroid.

5. Transition amplitude wave as a quasiparticle

We now come to what may be regarded as a physical interpretation of the ‘transition amplitude wave’. It was explained that TAW is generated through a total energy conserving (internally) inelastic scattering whereby the particle is excited by one or more Landau level intervals ($n \geq 1$), at the expense of the energy in the parallel component. The total energy conservation then yields

$$\frac{p^2}{2m} = \frac{p'^2}{2m} + n\hbar\Omega, \tag{25}$$

where p and p' are pre- and post-scattering parallel momenta, and $n\hbar\Omega$ is the change in the perpendicular energy corresponding to n Landau intervals. If we assume $p^2/2m \gg n\hbar\Omega$ (justifiably), then $p' \sim p$, and eq. (25) yields

$$k - k' = \frac{(p - p')}{\hbar} \simeq \frac{n\Omega}{v} = \kappa_n, \tag{26}$$

with $v = p/m$ being the parallel velocity.

We recall from the derivation of TAW in refs [7,10] that (26) is the defining relation for the TAW wave number which was found to be $\kappa_n = n\Omega/v$. In fact, essentially the same equation (25) was used to obtain (26) in refs [7,10]. If we now read eq. (26) as

$$p = p' + \frac{n\hbar\Omega}{v} \quad (27)$$

then (25) and (27) may be regarded as energy–momentum conservation relations for the parallel guiding centre motion, with $n\hbar\Omega$ being the energy complement, and $n\hbar\Omega/v$, the momentum complement. In fact, since $n\hbar\Omega/v$ represents the momentum of TAW, the energy–momentum packet $(\epsilon, \varpi) \equiv (\hbar\Omega, \hbar\Omega/v)$ for $n = 1$ may be assigned the identity of a ‘quasiparticle’ for the parallel dynamics, for which one has the relation $\epsilon = v\varpi$, or $\Omega = \kappa v$. (For $n > 1$ it may be regarded as a multiparticle excitation of n quasiparticles.) It follows that the phase velocity as well as the group velocity of the quasiparticle is v , the parallel velocity of the particle, that is, the quasiparticle co-moves with the real particle – the electron. This quasiparticle has been designated as ‘transiton’.

One thus has the following scenario: A charged particle in a magnetic field undergoes an inelastic scattering (internally) leading to an excitation of the particle to a higher Landau level by, in general, a level interval $n \geq 1$, at the expense of energy in its parallel motion by an amount $n\hbar\Omega$. Since the energy deficit $n\hbar\Omega \simeq n \cdot 10^{-6}$ eV (for $\mathcal{E} = 1$ keV, $B = 100$ G) is rather small, the particle would continue to execute its classical trajectory with only a small redistribution of energy between its parallel and perpendicular components, so that the trajectory remains almost intact. It is still described by the Lorentz dynamics. This would be in accordance with the current picture of the charged particle dynamics.

In the new picture, on the other hand, the energy–momentum packet (ϵ, ϖ) defined by the energy–momentum deficit caused by the scattering, itself acquires a physical identity as a ‘quasiparticle’ which co-moves with the particle trajectory. As has been demonstrated through a number of observations over the years [8–12], this quasiparticle has its manifestations in terms of the macroscale interference effects that have been accounted for by it. The proposed detection of the curl-free vector potential (on the macroscale) too, is attributed to the quasiparticle – the ‘transiton’. An experimental substantiation of this effect with its various unanticipated and novel characteristics will lead to a further confirmation of the physical reality of the ‘transition amplitude wave’. This in turn would help establish a new paradigm: According to it, the scattered particle in an inelastic scattering is not just scattered away with a diminished/enhanced energy–momentum, but in a significant new twist also carries a ‘memory’ of its immediate past post-scattering transition in terms of the actual energy deficit/gain it has suffered in the process. The ‘transiton’ carries that information which leads to the macroscale quantum effects. Such a ‘memory effect’ does not exist in the conventional picture.

This represents the most fascinating revelation of these investigations at the conceptual level, namely, that a quantum transition in the bound perpendicular degree of freedom should leave a signature in the parallel (free) degree of freedom. This signifies an essential characteristic quantum property of ‘connectedness’.

On the formal level, the existence of a quantum object like the ‘transiton’ sharing the Hamiltonian flow of the classical trajectory is reminiscent of the Koopman theorem [13]. This states that if one attaches an element $\varphi(A)$ of a Hilbert space \mathcal{H} to a point A of the phase space \mathcal{P} of a dynamical system, then $\varphi(A)$ undergoes a

unitary transformation – an automorphism of \mathcal{H} which is induced by the Hamiltonian flow of the phase space \mathcal{P} . With reference to our system the ‘transiton’ belongs to a Hilbert space and the charged particle trajectory defines the Hamiltonian flow. The parallel is obvious, and one may well regard the case in point to exemplify the Koopmanian flow.

6. Summarizing comments

As is well known, the detection of a curl-free vector potential in quantum systems, referred to as the Aharonov–Bohm effect [1], was brought to light not before nearly a couple of decades since the advent of quantum mechanics. It was then considered a rather dramatic revelation, though its acceptance was not entirely smooth. (See, for example ref. [15] for a glimpse of the situation prevailing around that time.) The detection of the curl-free vector potential on the macroscale proposed here could be even more discomfiting, because it would appear to come into conflict with the current, well-accepted conceptual framework whereby charged particle dynamics on the macroscale ought to be ‘necessarily and sufficiently’ describable by the classical Lorentz equation, and moreover, a curl-free magnetic vector potential could have no physical significance on the macroscale, since the associated field, which alone is recognized as an observable in classical electrodynamics, vanishes. It is therefore necessary to first reassure that the above-mentioned observation, however unusual it may be, poses no conflict of the above sort.

The resolution, as elaborated extensively in §5, lies in the fact that the various macroscale matter wave effects, predicted and observed, including the present one under discussion, are to be traced to the dynamics not of the particle, but of the new quantum entity, which is on the macroscale with an \hbar -independent wavelength and which does not involve the particle mass explicitly. It has been assigned an identity as a quasiparticle – christened as the ‘transiton’ which corresponds to an energy–momentum ‘hole’ in the guiding centre trajectory. It has a quantized energy $\hbar\Omega$ associated with it which corresponds to the excitation energy across one Landau level.

On the other hand, the well-known classical and quantum dynamical effects are associated with the real particle and involve the particle mass explicitly (e.g. de Broglie wavelength and Lorentz equation of motion). Moreover, the excitation of a ‘transiton’ in the guiding centre trajectory involves, as pointed out already, such a tiny redistribution of energy ($\sim 10^{-6}$ eV) that it does not affect the course of the charged particle trajectory in any significant manner. This means that the classical charged particle dynamics remains unaffected by the ‘transiton’ dynamics. In fact, the ‘transiton’ is itself transported by the charged particle trajectory which is yet governed by the Lorentz equation. It leads to a rather peculiar situation, that a structure – the TAW – riding ‘piggyback’ on the classical trajectory imparts to it a macroscale quantum character which is entirely distinct from the well-known microscale one, but does not affect the classical or the quantum dynamics of the particle itself.

Also, this quasiparticle is distinct from other known quasiparticle excitations, e.g. phonons in quantum fluids. The latter ones have a phase velocity which is determined by the medium properties (like sound waves) independently of the fluid velocity. The phonon linear dispersion relation then connects its frequency and wave number through the sound speed as its phase velocity, and has, in principle, a continuous spectrum. This is in contrast with the ‘transiton’ where its phase velocity is the particle velocity itself since it co-moves with the particle trajectory that it is excited in. Here the frequency is specified by the Landau level intervals defining the transitions, and the wave number is determined by its frequency through the particle velocity as its phase velocity. Because of the discreteness of the Landau level intervals, this quasiparticle has a discrete spectrum in energy, and hence in wave number. This has, in fact, been demonstrated in the experiments reported in [11].

We have thus advanced herein an entirely novel concept of quasiparticle excitation in a particle trajectory which has not been proposed earlier to the best of author’s knowledge. It may also be added that this concept has a more general applicability than just for charged particle dynamics. It can be applied to any bound system, like atoms and molecules, where the centre of mass motion serves as the unbound degree of freedom, and the quasiparticle excitation occurs in the latter, consequent to an excitation in its bound degrees of freedom. The author has in fact considered these systems as well [16].

We next comment on the unusual one-dimensionality of the macroscale vector potential observation. As we have noted, the latter observation is much more richer in its physical content than the corresponding microscale effect – the AB effect. The one-dimensionality of the effect which is obviously contrary to the generally held understanding of the vector potential observation prejudiced through the AB effect, hinges on the mechanism of generation of the TAW and its point of origin, and the fact that path lengths traversed by the TAW are then naturally reckoned from their points of origin. This enables a path difference to be generated in one dimension which the curl-free vector potential is integrated over, and the line integral is subsequently evaluated in terms of the flux trapped in the torus. Note that the path difference (x_o, x_g) between (x_o, x_p) and (x_g, x_p) is an open path as are the latter. This would appear to pose a quandary with respect to the question of gauge invariance of the line integral over the open path. In the case of the AB effect the circuit integral involved in it is manifestly gauge invariant. The subtle question of gauge invariance in the present case is discussed in the text.

One ought to emphasize the importance of the condition which must be satisfied to be able to observe the effect as stipulated. This relates, as already explained, to the tuning of the magnetic field (for a given energy and gun–grid distance) such that it corresponds to an interference maximum. Without such a tuning, one will not observe well-formed maxima/minima in the detector plate current with the variation of the current in the toroidal solenoid as reported above.

Clearly, there are a number of characteristic features of this proposed effect which are quite heterodox in many respects. These have been demonstrated above to have their origin in the novel ‘quasiparticle’ excitation advanced here. This concept has led to an entirely new physics whereby one has a whole class of physical phenomena which exhibit matter wave characteristics on the macroscale. Some of these have

already been established [9–11]. However, the effects (vector potential observation) predicted and proposed currently would be by far the most unusual. While some aspects of this effect have already been checked [12], some others discussed here are rather crucial in establishing the above concept. We have been carrying out experiments to check these additional features, for which we have found the evidence. We should be communicating these results shortly [14].

It is, however, important to emphasize that the existence of these macroquantum effects do not in any way negate either the existence of the classical trajectory or the quantum character (like the de Broglie waves) associated with it. We thus have a rather unique situation where the trajectory *à la* classical dynamics coexists with a quantum attribute – the ‘transiton’ – leading to the quantum effects on the macroscale associated with the trajectory. By the same token, it also implies the coexistence of matter wave effects on two distinct spatial scales (microscale *à la* de Broglie, and macroscale *à la* ‘transiton’) separated by several orders of magnitude.

Finally, to avoid any possible misunderstanding that may yet linger as to the nature of the formalism and the effects emanating from it, it is important to re-emphasize that the latter are really of quantum origin, since eqs (1) and (3) governing them have been derived in refs [6] and [7] using the Schrödinger equation in the Feynman path integral representation. The formalism is therefore NOT ‘quantum-like’ as some readers might be led to believe, but a derivative of quantum mechanics itself.

Appendix A

The interference term in eq. (9) corresponds to the phase difference between the two paths (x_o, x_p) and (x_g, x_p) with the phase of the form $[\frac{1}{\mu} \int dx (mv + \frac{e}{c} A)]$, where μ is the initial value of the gyroaction ($\mu = \mathcal{E} \sin^2 \delta / \Omega$). In an experiment there is usually a small spread $\Delta\mu$ centred around a mean $\bar{\mu}$. To take account of this spread we first rewrite eq. (9) in the form

$$|\Psi(x_p)|^2 = \alpha_1^2 + \alpha_2^2 + 2\alpha_1\alpha_2 \cos \left[\frac{n}{\mu} \left\{ \int_{x_o}^{x_g} dx \left(mv + \frac{e}{c} A_x \right) - 2\pi k\mu \right\} \right]. \quad (\text{A1})$$

This form also leads to the same condition for the maxima of the interference term, namely, $\int_{x_o}^{x_g} n(mv + \frac{e}{c} A_r) = 2\pi k\mu$, as the form (9).

We next integrate (A1) over the small spread $\Delta\mu$ in μ . This is similar to the integration of a wave function for a dispersive wave carried out over a small spread Δk in the wave number k . This, as we know, leads to the construction of a wave packet and the definition of the group velocity of the dispersive wave. We anticipate a similar group-like property to emerge from the integration of (A1) over the spread $\Delta\mu$. To integrate (A1) with an appropriate distribution $f(\mu)$ expand the argument of the cosine function in (A1) around $\bar{\mu}$ (recall that $v = [2(\mathcal{E} - \mu\Omega)/m]^{1/2}$), we have (denoting $\bar{v} = [2(\mathcal{E} - \bar{\mu}\Omega)/m]^{1/2}$) on integrating with respect to μ

Nature of the transition amplitude wave

$$\begin{aligned}
 & \int d\mu f(\mu) |\Psi(x_p, \mu)|^2 \\
 & \equiv \langle |\Psi(x_p, \mu)|^2 \rangle \\
 & = \alpha_1^2 + \alpha_2^2 + 2\alpha_1\alpha_2 \int \cos \left[\frac{n}{\bar{\mu}} \left\{ \int_{x_o}^{x_y} dx \left(m\bar{v} + \frac{e}{c} A_x \right) \right. \right. \\
 & \quad \left. \left. + 2\pi k\bar{\mu} + (\mu - \bar{\mu}) \int_{x_o}^{x_g} dx m \frac{\partial v}{\partial \mu} \Big|_{\bar{\mu}} \right. \right. \\
 & \quad \left. \left. - 2\pi k(\mu - \bar{\mu}) \right\} \right] f(\mu) d\mu. \tag{A2}
 \end{aligned}$$

If we expand the cosine term which has the form $\cos[g(\bar{\mu}) + (\mu - \bar{\mu})\partial g/\partial \bar{\mu}]$ using the trigonometric identity, the $\sin[(\mu - \bar{\mu})\partial g/\partial \bar{\mu}]$ term being odd in $(\mu - \bar{\mu})$ vanishes on integration with the even function $f(\mu)$. The remaining term yields

$$\begin{aligned}
 \langle |\Psi(x_p, \mu)|^2 \rangle & = \alpha_1^2 + \alpha_2^2 \\
 & + 2\alpha_1\alpha_2 \int \cos \left\{ \frac{n}{\bar{\mu}} \int_{x_o}^{x_g} dx \left(m\bar{v} + \frac{e}{c} A_x \right) - 2\pi k \right\} \\
 & \int d\mu \cos \left\{ n \frac{(\mu - \bar{\mu})}{\bar{\mu}} \left[\int_{x_o}^{x_g} dx m \frac{\partial v}{\partial \mu} \Big|_{\bar{\mu}} - 2\pi k \right] \right\} f(\mu) d\mu \\
 & = \alpha_1^2 + \alpha_2^2 + 2\alpha_1\alpha_2 \cos \left\{ \frac{n}{\bar{\mu}} \left[\int_{x_o}^{x_g} \left(m\bar{v} + \frac{e}{c} A_x \right) dx - 2\pi k\bar{\mu} \right] \right\} \\
 & \times F(X) \tag{A3}
 \end{aligned}$$

with

$$F(X) = \exp \left[- \left(\frac{1}{2\beta\bar{\mu}} X \right)^2 \right], \tag{A4}$$

where we have used $(m\partial v/\partial \mu) = \Omega/\bar{v}$ to obtain the last form in (A4), and the distribution $f(\mu)$ is assumed here to be a Gaussian

$$f(\mu) = \frac{\beta}{\sqrt{\pi}} \exp[-\beta^2(\mu - \bar{\mu})^2] \tag{A5}$$

and where

$$X \equiv \left[\int_{x_o}^{x_g} n \frac{\Omega dx}{\bar{v}} - 2\pi k \right]. \tag{A6}$$

Because of the form $\exp[-(X/2\beta\bar{\mu})^2]$ of the factor $F(X)$, the interference term has its maximum amplitude for $X = 0$, and rapidly becomes small as X departs from zero. The relation, $X = 0$, that is,

$$\int_{x_o}^{x_g} n \frac{\Omega dx}{\bar{v}} - 2\pi k = 0, \quad k = 1, 2, 3, \tag{A7}$$

thus corresponds to a group-like condition for the interference maxima for $k = 1, 2, 3, \dots$. We note that the smaller is the value $(\beta\bar{\mu})$, the more sharp is the amplitude factor $F(X)$ peaked around $X = 0$, and more rapidly it goes to zero as X departs from zero (that is the condition (A7)). Thus, the ‘group’-quantum condition (A7) would effectively represent the condition for one-dimensional interference maxima. Note that the condition (A7) does not involve the vector potential A , but the cosine factor does contain A in its argument.

Appendix B

The dependence of $\Delta\Phi$ on $1/G$ is found to be most dramatic as the grid is moved across the position of toroid’s centre. We note that when the position z_g of the grid Q is on the left-hand side of the core as shown in figure 1, $\theta_1^{(g)}$ and $\theta_2^{(g)}$ are both $< \pi/2$. When Q crosses the point z_1 , $\theta_1^{(g)} > \pi/2$. Likewise $\theta_2^{(g)} < \pi/2$ when $z_g < z_2$ and $\theta_2^{(g)} > \pi/2$ when $z_g > z_2$.

The experiment is to be carried out by varying the position of the grid from the one on the left-hand side of the core ($z_g < z_1, z_2$) through the core ($z_2 > z_g > z_1$) and to the other side ($z_g > z_1, z_2$). It will be noticed that the variation in the value of G is maximum as z_g goes through the core ($z_2 > z_g > z_1$) from a value $(r_o/\ell_o)[\text{cosec } \hat{\theta}_2^{(g)} - 1 - q(\theta_1^{(o)}, \theta_2^{(o)})]$ at $z_g = z_1$ (where $\theta_2^{(g)} = \tan^{-1}(r_o/\ell_o)$), to the value $(r_o/\ell_o)[1 - \text{cosec } \hat{\theta}_1^{(g)} - q(\theta_1^{(o)}, \theta_2^{(o)})]$, at $z_g = z_2$, the total change being $\Delta G = 2r_o/\ell_o$. Here $q(\theta_1^{(o)}, \theta_2^{(o)}) = \text{cosec } \theta_2^{(o)} - \text{cosec } \theta_1^{(o)}$.

We now proceed to examine the dependence on the geometrical factor G through the angles $\theta_1^{(g)}$ and $\theta_2^{(g)}$ where

$$\begin{aligned} \theta_1^{(g)} &= \tan^{-1} \left[\frac{r_o}{(z_1 - z_g)} \right], & \theta_1^{(g)} &\leq \pi/2 \\ &= \tan^{-1} \left[\frac{r_o}{(z_g - z_1)} \right], & \theta_1^{(g)} &> \pi/2 \end{aligned} \tag{B1}$$

$$\begin{aligned} \theta_2^{(g)} &= \tan^{-1} \left[\frac{r_o}{(z_2 - z_g)} \right], & \theta_2^{(g)} &\leq \pi/2 \\ &= \tan^{-1} \left[\frac{r_o}{(z_g - z_2)} \right], & \theta_2^{(g)} &> \pi/2. \end{aligned} \tag{B2}$$

It easily follows that

$$\text{cosec } \theta_1^{(g)} = \left\{ 1 + \frac{1}{r_o^2} \left[\frac{1}{2}(L - \ell_o) - D \right]^2 \right\}^{1/2} \tag{B3}$$

$$\text{cosec } \theta_2^{(g)} = \left\{ 1 + \frac{1}{r_o^2} \left[\frac{1}{2}(L + \ell_o) - D \right]^2 \right\}^{1/2}. \tag{B4}$$

Nature of the transition amplitude wave

Using the definition of G as implied in eq. (24) we have $G = (r_o/\ell_o)f(\theta)$ where $f(\theta)$ is given by

$$f(\theta) = [\operatorname{cosec} \theta_2^{(g)} - \operatorname{cosec} \theta_1^{(g)} - q(\theta_2^{(o)}, \theta_1^{(o)})] \quad (\text{B5})$$

with $q(\theta_1^{(o)}, \theta_2^{(o)}) = \operatorname{cosec} \theta_2^{(o)} - \operatorname{cosec} \theta_1^{(o)}$. Note that $\operatorname{cosec} \theta_2^{(o)} = \operatorname{cosec} \theta_1^{(g)}$ for $D = 0$ if the source (the gun) and the plate are symmetrically placed with respect to the toroid.

References

- [1] Y Aharonov and D Bohm, *Phys. Rev.* **115**, 485 (1959)
- [2] R G Chambers, *Phys. Rev. Lett.* **5**, 3 (1960)
- [3] A Tonomura, N Osakaba, T Matsuda, J Kawasaki, J Endo, S Yane and H Yamada, *Phys. Rev. Lett.* **56**, 792 (1986)
- [4] R K Varma, *Phys. Rev. Lett.* **26**, 417 (1971)
- [5] R K Varma, *Phys. Rev.* **A31**, 3951 (1985)
- [6] R K Varma, *Phys. Rev.* **E64**, 036608-(1-10) (2001); Erratum: *Phys. Rev.* **E65**, 019904 (2002)
- [7] R K Varma, *Pramana - J. Phys.* **68**, 901 (2007)
- [8] R K Varma, *Phys. Rep.* **378**, 301 (2003)
- [9] R K Varma and A M Punithavelu, *Mod. Phys. Lett.* **A8**, 167 (1993)
- [10] R K Varma, A M Punithavelu and S B Banerjee, *Phys. Rev.* **E65**, 026503-(1-9) (2002)
- [11] R K Varma and S B Banerjee, *Phys. Scr.* **75**, 19 (2007)
- [12] R K Varma, A M Punithavelu and S B Banerjee, *Phys. Lett.* **A303**, 114 (2002)
- [13] B O Koopman, *Proc. Natl. Acad. Sci. (U.S.A.)* **17**, 315 (1931)
- [14] R K Varma, S B Banerjee and A Ambastha, to be communicated
- [15] D Home and S Sengupta, *Am. J. Phys.* **51**, 942 (1983)
- [16] R K Varma, *Eur. Phys. J.* **D20**, 211 (2002)